LAWRENCE
LIVERMORE
NATIONAL
LABORATORY

LLNL-TR-459199

DOE International Collaboration; Seismic Modeling and Simulation Capability Project

L. D. Leininger, R. R. Settgast

October 13, 2010

Disclaimer

This work performed under the auspices of the U.S. Department of Energy by Lawrence Livermore National Laboratory under Contract DE-AC52-07NA27344.

Lawrence Livermore National Laboratory

COMPUTATIONAL GEOSCIENCES GROUP

UCRL-TR-459199

FINAL REPORT

Seismic Modeling and Simulation Capability Project

DOE International Collaboration

US-Japan Joint Nuclear Action Plan (JNEAP)

October 1, 2010

Prepared for:

DOE NEAMS Program Office

Prepared by:

Lara Leininger, Ph.D. and Randolph Settgast, Ph.D.

(925) 423-6573

lara@llnl.gov

This work performed under the auspices of the U.S. Department of Energy by
Lawrence Livermore National Laboratory under Contract DE-AC52-07NA27344

P.O. Box 808 Livermore, California 94551-0808 • Telephone (925) 422-1100 • http://www.llnl.gov

EXECUTIVE SUMMARY

The following report describes the development and exercise of a new capability at LLNL to model complete, non-linear, seismic events in 3-dimensions with a fully-coupled soil structure interaction response. This work is specifically suited to nuclear reactor design because this design space is exempt from the Seismic Design requirements of International Building Code (IBC) and the American Society of Civil Engineers (ASCE) [4,2]. Both IBC and ASCE-7 exempt nuclear reactors because they are considered "structures that require special consideration" and their design is governed only by "other regulations". In the case of nuclear reactors, the regulations are from both the Nuclear Regulatory Commission (NRC) [10] and ASCE 43 [3]. This current framework of design guidance, coupled to this new and evolving capability to provide high fidelity design solutions as presented in this report, enables the growing field of Performance-Based Design (PBD) for nuclear reactors subjected to earthquake ground motions.

As part of the capability development, the project team implemented a novel non-linear soil model which has been developed for cyclic (seismic) loading and parameterized for relevant in-situ sand. Through a series of complex evolution equations and material parameters, this model gives the team the capability to predict the onset of liquefaction – the geologic phenomena implicated when a saturated soil under cyclic loading suddenly (or in the timescale of minutes) loses its shear capacity and begins to respond like a fluid. This model shows great promise in evolving the project to the next phases which are full-scale validation and, ultimately, high-fidelity predictive modeling for PBD.

Also as part of the capability development, numerous computational geometries were developed to test certain physical aspects of the seismic response. These models ranged in fidelity from single element representations to full 3-dimensional soil coupled to structures. Each model was used to test aspects of the soil representation as well as to establish computational and geometric uncertainty. This comprehensive approach to uncertainty quantification ensures the robustness of any application for PBD.

The final product demonstrates that we have a high-fidelity and robust capability to model seismic events and structural response within LLNL's ALE3D. Future work will be to validate the soil model with experimental data on sand from colleagues at UC Davis and to collaborate our work and experience with the International Atomic Energy Agency (IAEA) and the Japanese Atomic Energy Agency (JAEA) as part of a growing international collaboration.

TABLE OF CONTENTS

PROJECT OVERVIEW

On July 16, 2007, a magnitude 6.8 (M6.8) earthquake struck in the Sea of Japan and was followed by a M6.6 earthquake off the West Coast of Honshu. The epicenters of these seismic events were in close proximity to Tokyo Electric Power Company's (TEPCO) Kashiwazaki-Kariwa Nuclear Reactor Facility. A USGS Shake Map indicates that the region where the plant resides experienced "strong perceived shaking" as a result of the M6.6 Honshu event. The ground motion induced by the events was in excess of the Design Basis for reactor facilities in Japan – the same Design Basis that is used in the United States. According to news reports, these events developed ground motion sufficient to cause approximately 1.5 liters of radioactive water to spill out of a cooling pond for spent fuel rods at one of TEPCO's reactors.

This event gave rise to concern within the nuclear safety community and discussion that improvements should be evaluated to validate United States design methods, which are used across the world. It was discussed at the U.S.-Japan Nuclear Energy Steering Committee (March 19, 2010) that the risk associated with damage from a seismic event is so great that it justifies the application of high-fidelity computational modeling and simulation. As such, cooperative research between the two countries on advanced simulation is essential for enhanced seismic safety of reactor facilities.

Lawrence Livermore National Laboratory (LLNL) has existing 3-dimensional finite element modeling tools, ALE3D [1] and Diablo [7], which have been developed over decades with Department of Energy (DOE) funding. ALE3D is the state-of-the-art in computational fluid dynamics, shock-wave propagation and fluid-structure interaction. Diablo is the preeminent non-linear implicit structural mechanics capability at LLNL which enables massively parallel simulations of acoustic/seismic waves and structural response. This project leverages the tremendous development efforts of the DOE and others to develop the capability within ALE3D and Diablo to model seismic events.

The initial phase of this project (discussed in this report) has demonstrated the capability of LLNL's ALE3D hydrodynamic code to propagate seismic events with non-linear soil models. Follow-on work will validate the soil model to laboratory data, enable the modeling of pore-pressure dissipation (which can lead to longer time scale liquefaction), implement implicit solution techniques, and further develop the collaboration with Japanese scientists and engineers. The final phase will use ALE3D and Diablo to couple the seismic event to as-built reactor structures based on data from the Kashiwazaki event.

This phased and directed work is essential for the thorough validation and verification of the software for applications in the seismic regime. This will directly lead to the development of Design Basis for nuclear reactors to ensure the safety of the world's greenest and most reliable energy source. The results will be shared and collaborated with our Japanese colleagues to promote the seismic safety of these structures.

Achievements in Phase 1

In FY10 this project completed its Phase 1 tasks which demonstrated the capability of modeling a seismic event through drained and undrained soil and the soil-structure interaction of a notional nuclear reactor using explicit hydrodynamics. In this phase, the work had been focused on testing a novel soil model implementation, SANISAND [8], as well as investigating boundary and loading condition sensitivities. The results of Phase 1 will be coordinated with the US-Japan Nuclear Energy Steering Committee Simulation & Modeling Working Group and presented at a conference in Japan, the *1st Kashiwazaki International Symposium on Seismic Safety of Nuclear Installations,* in November 2010. As part of our collaboration, the Japanese are expected to support our entry into the IAEA's Kashiwazaki-Kariwa Research Initiative for Seismic Margin Assessment (KARISMA) benchmark collaboration so that we can acquire site and structural data from the July 2007 seismic event including damage recordings at the Kashiwazaki-Kariwa Nuclear Reactor Facility.

The project approach incorporated numerous computational geometries to test certain physical aspects of the seismic response. These models are shown in Figure 1 and they ranged in fidelity from single element representations to full 3-dimensional coupled to structures. Each model was used to test aspects of the soil model as well as computational and geometric uncertainty. This approach to uncertainty quantification ensures the robustness of any application for Performance-Based Design.

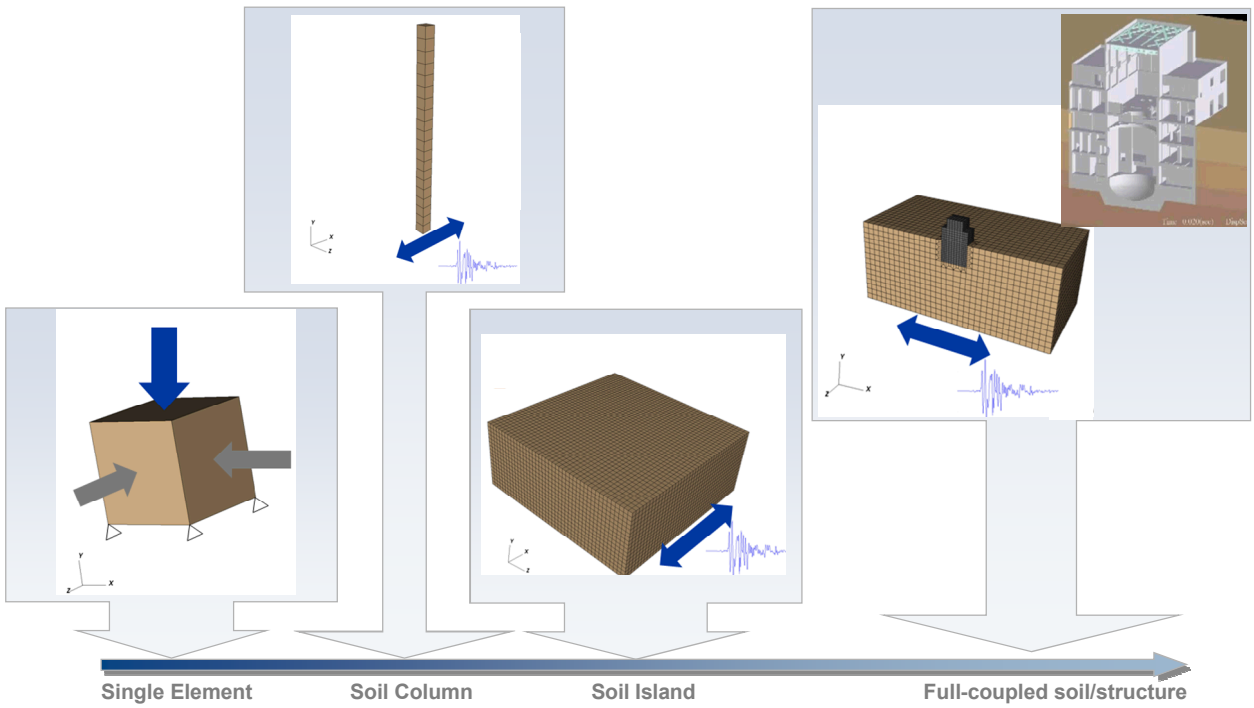

Figure 1: A phased approach is applied to enhance the verification process with a range of finite element models of increasing complexity.

Seismic Loading

When this project was initiated, the ground motion data from the July 2007 event at the Kashiwazaki-Kariwa Nuclear Reactor Facility was not publically available. There were two seismic events with epicenters near the plant, and they struck hours apart on July 16, 2007. First, a M6.8 earthquake struck in the Sea of Japan and was followed by a M6.6 earthquake off the West Coast of Honshu. A USGS Shake Map indicates that the region where the plant resides experienced "strong perceived shaking" as a result of the M6.6 Honshu event (see Figure 2).

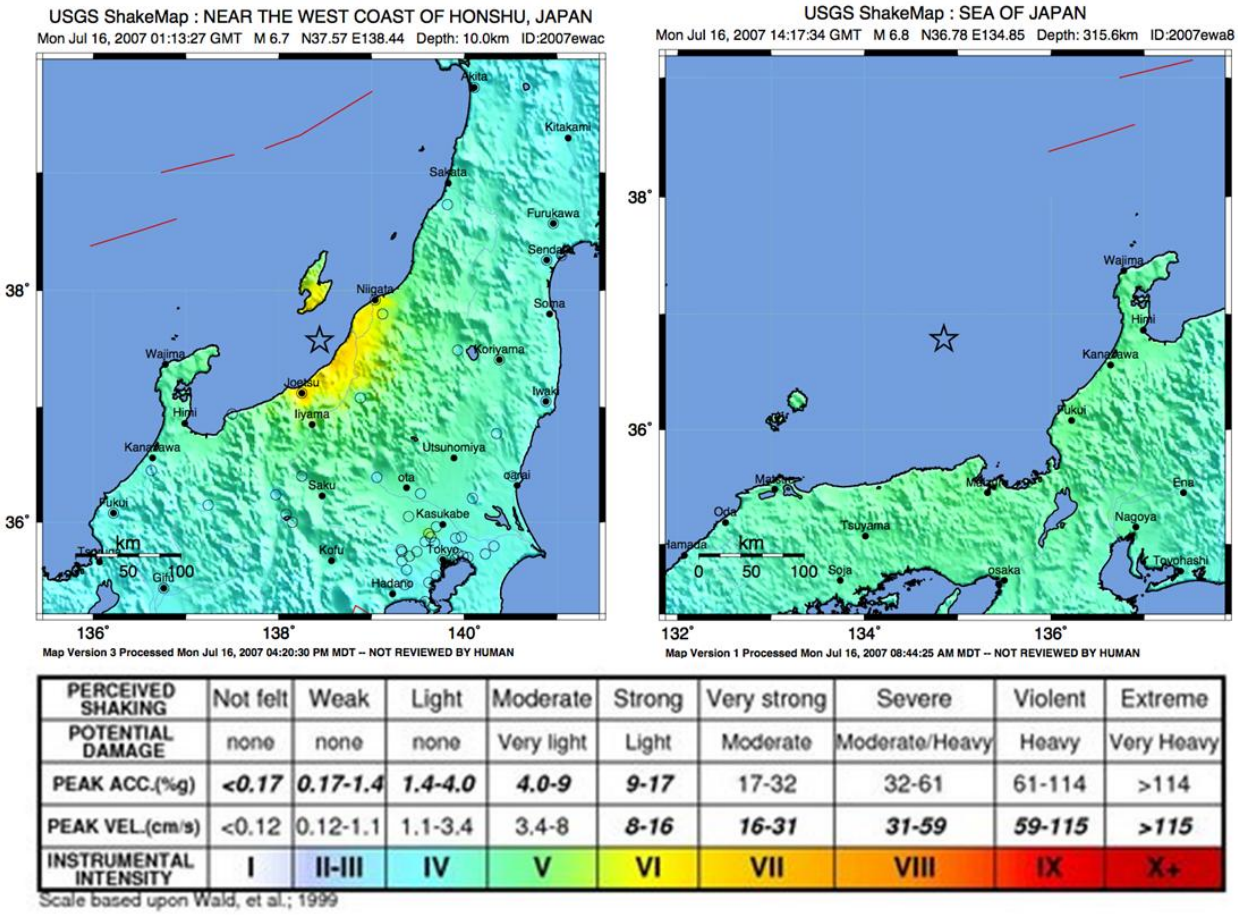

Figure 2: USGS ShakeMaps of the July 16, 2007 seismic events in Honshu and the Sea of Japan [9]

In order to develop a representative approximation we looked through the large repository of data available from the 1995 Kobe earthquake which was a M6.9. Our intent was to find ground motion records from Kobe at approximately the same distance from the epicenter as the Honshu epicenter to the Kashiwazaki-Kariwa Nuclear Reactor Facility. The approximate distance from the epicenter of the Honshu event and the Facility is 24 km with a Hypocentral distance of 29 km. We found ground motion records from the Kobe event at a Hypocentral distance of approximately 26 km. These motions give a peak velocity of 32 in/sec and a peak displacement of 6.8 in, and they are shown in Figure 3.

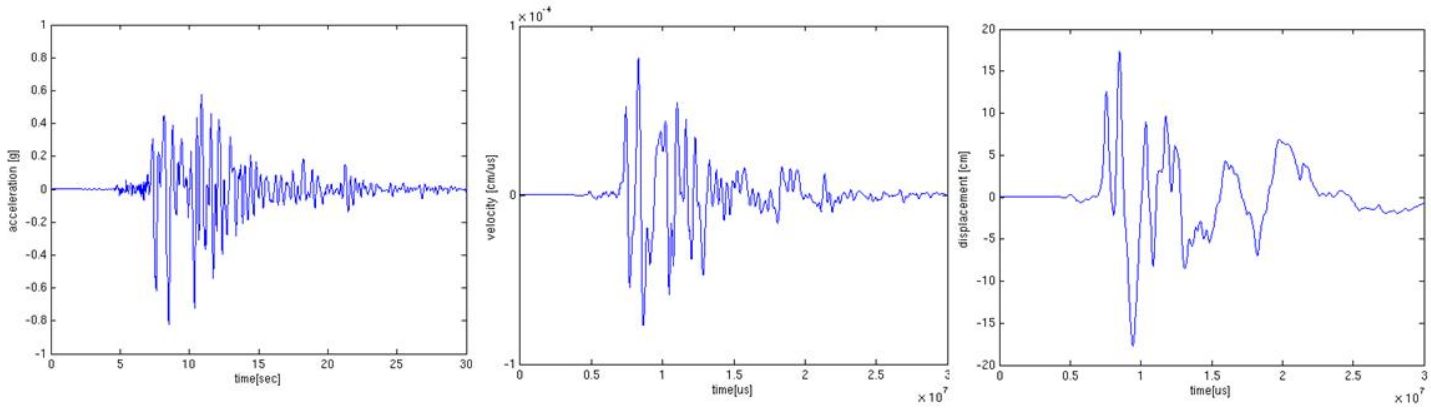

Figure 3: Earthquake ground motions from the M6.9 Kobe event (1995) at 26 km from the Hypocenter

SANISAND Non-linear Constitutive Model

SANISAND has been developed at UC Davis as a collaboration between numerous professors and graduate students. The version that has been implemented into ALE3D is published by Taiebat and Dafalias [8]. SANISAND has a demonstrated capability to evolve plasticity under cyclic loading and it is valid in the critical state (e.g. during liquefaction); making it a perfect fit for our project.

Figure 4 shows a schematic of the single element tri-axial compression tests that were used to verify the soil model for drained and undrained response using the published data for Toyoura sand [8]. In this model, axial load was applied in the Y-direction and confinement pressure was applied in the X and Z directions.

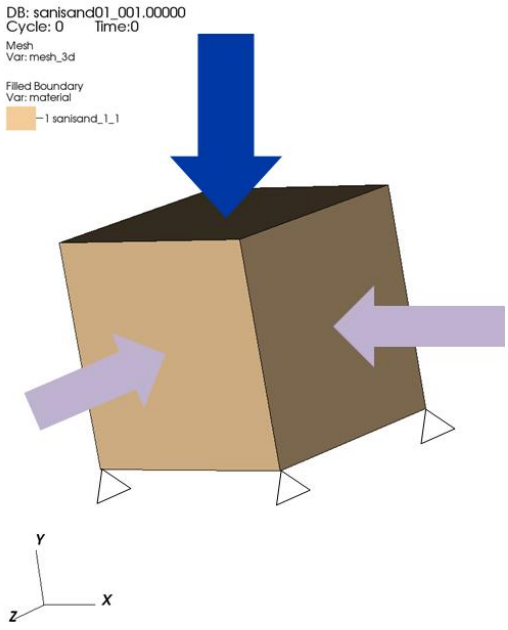

Figure 4: Single-element model used for model verification of SANISAND

The published data looked at the undrained (saturated) response of the soil for a range of void ratios from 0.735 and 0.907. The data also looked at the drained (unsaturated) response for initial void ratios between 0.809 and 0.960. Figure 5 shows a comparison of the undrained response for three representative void ratios, while Figure 6 shows comparisons for the drained response. In all the plots, the solid lines are the ALE3D results and the symbols are the data from the literature.

In all cases, the ALE3D implementation closely follows the SANISAND data from the paper. Moving forward with our calculations for earthquake-induced liquefaction, we will use only the saturated soil model as the fully saturated soil response during seismic ground motion would give the worst-case scenario for maximum structural damage.

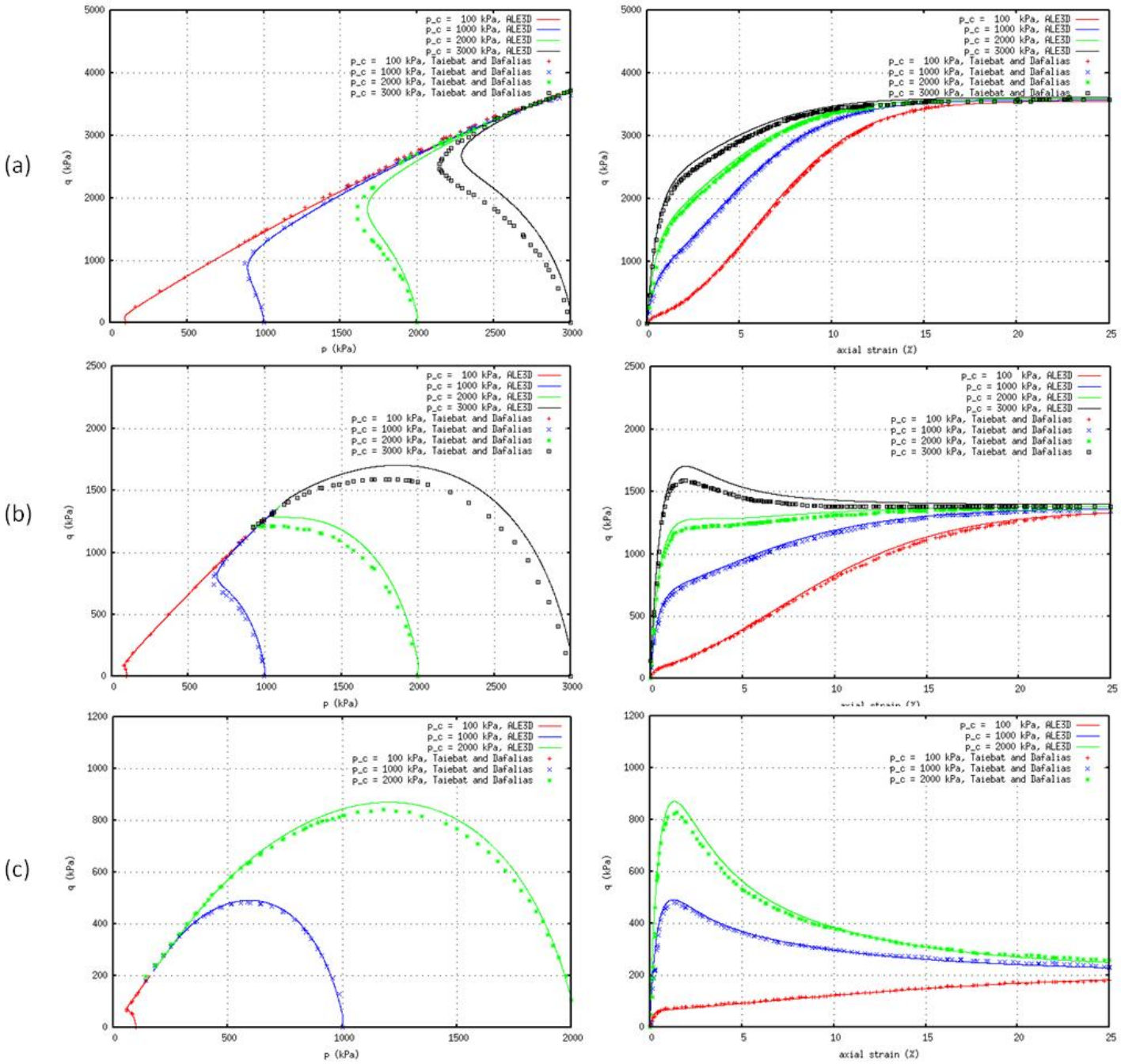

Figure 5: Deviatoric stress, q [kPa], as a function of confining pressure, p [kPa], and axial strain % for tri-axial tests of various undrained (saturated) soil samples at varying compactions ($100 \le p_c \le 2000$ kPa): (a) dense soil with void ratio=0.735, (b) medium dense soil with void ratio=0.833, and (c) loose soil with void ratio=0.907. In all these plots, the solid lines are the ALE3D results and the symbols are the data from [8].

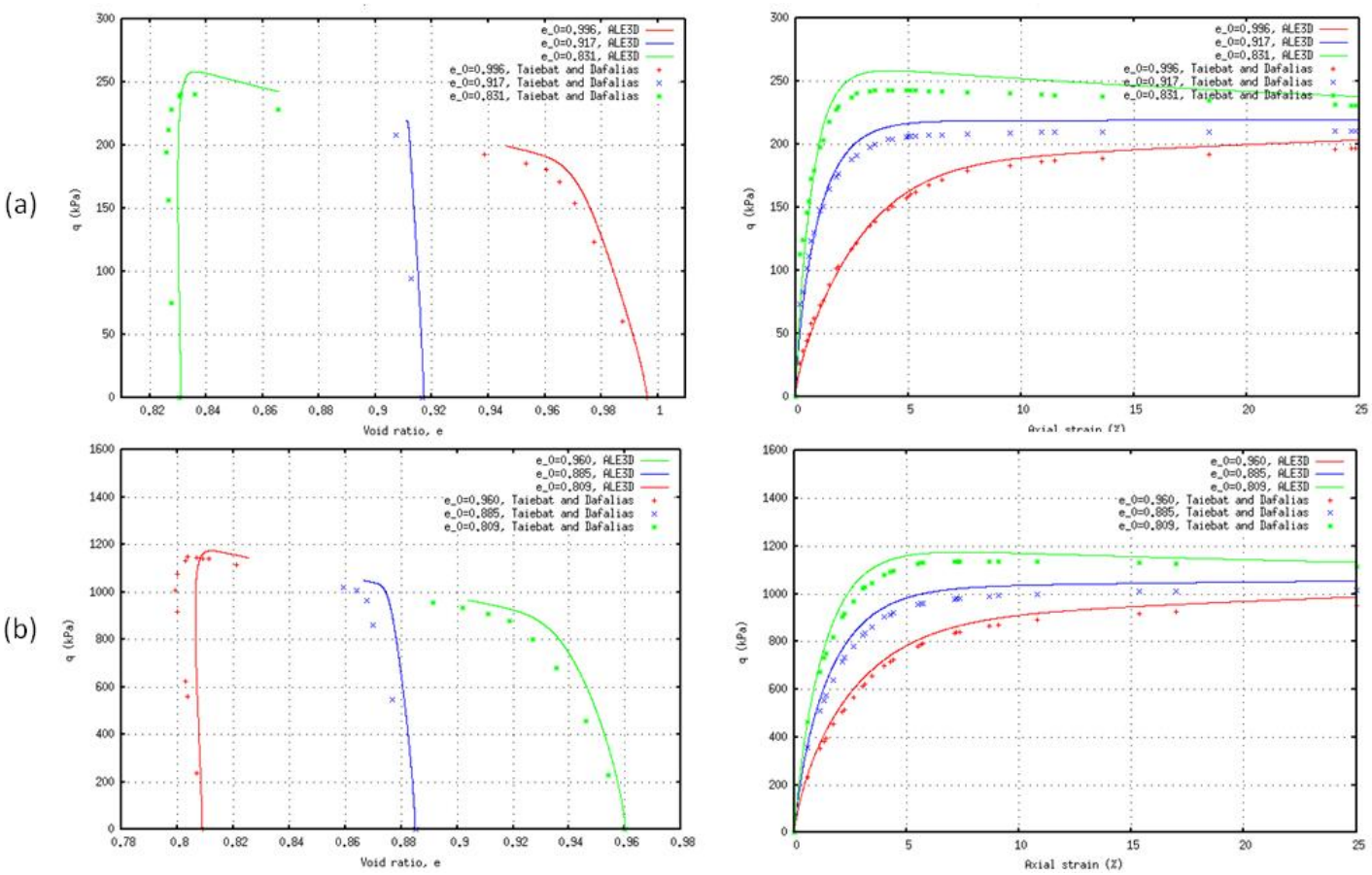

Figure 6: Deviatoric stress, q [kPa], as a function of void ratio, e, and axial strain % for tri-axial tests of drained (unsaturated) soil with various confining stresses ($0.809 \le e_0 \le 0.996$): (a) 100 kPa confinement (b) 500 kPa confinement. In all these plots, the solid lines are the ALE3D results and the symbols are the data from [8].

Liquefaction and Void Ratio Dependence

To test the response of the undrained model to an in-situ column of soil, a computational column model was constructed. Shown in Figure 7, the model was 200 cm wide and 2 m deep with a total of 20 elements. It takes only 7 minutes to run on a single processor, but scaling up to problems with 3-dimensional fidelity for soil-structure interaction (~10 million zones) would result in a run time of 2.5 days (24 hours a day) on 100 processors.

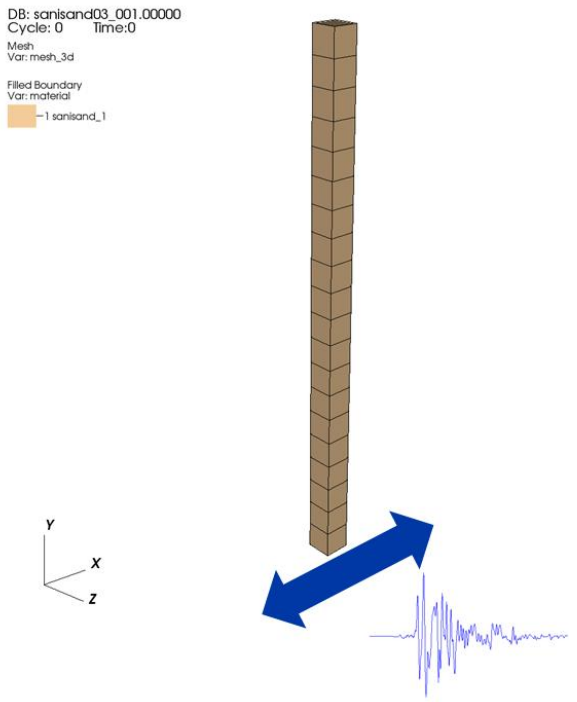

Figure 7: Soil-column model used to test liquefaction model and effects of void ratio on liquefaction with the SANISAND model

As previously mentioned, the SANISAND model helps us meet our project objective of simulating liquefaction. Liquefaction is a condition that occurs when the excess pore pressure exceeds the vertical stress from the overburden, and the contact forces between soil particles decreases to zero. With no appreciable normal force between soil particles, the soil loses its shear capacity. The buildup of pore water pressure typically results from shearing of a soil that is less dense than its so-called "critical state" at a given effective pressure. When subjected to bulk shear deformations, the soil particles will have a tendency to rearrange themselves to the density corresponding to critical state. However, the water that fills the pore space does not allow a volume change, and thus soil particles simply lose contact with each other. This phenomena can occur during a seismic event (in saturated soils) when the soil is subjected to shear loading, or it can occur minutes to hours after the even as a result of pore pressure dissipation through the porous soil (represented by Darcy Flow). The focus of this current capability is the instantaneous (during the event) liquefaction in saturated soils – disregarding Darcy Flow through the aquifer.

The liquefaction approximation applied here uses the pore pressure history variable available in the SANISAND model. This can be combined with the vertical stress to develop a relationship for the excess pore pressure ratio as shown in Eqn.1. The value of this ratio is expected to be zero (0) when there is no likelihood of liquefaction and one (1) when the soil is expected to liquefy.

$$r_u = \frac{u^e}{\sigma_{vo}'}$$

where:

r_u **=Excess Pore Pressure Ratio**

u_o **=Intial Pore Pressure**

u^e **=Excess Pore Pressure**

σ_v **=Total Vertical Stress**

σ_v' **=Effective Stress** $\left\{\sigma_v' = \sigma_v - (u_o + u^e)\right\}$

σ_{vo}' **= Inital Value of Effective Stress**

{1}

Using the dense sand model (void ratio, e, of 0.735) and the full-strength Kobe earthquake as a baseline, it was found that the entire column of soil is expected to liquefy. The magnitude of the earthquake was scaled to accommodate a scenario when only a part of the column experiences liquefaction. This is also a good test of the qualitative model behavior to ensure that the likelihood of liquefaction is reduced in the column as the ground motion is scaled down.

Figure 8 through Figure 11 show the results for this study. The scaling factor of 0.1 for the Kobe ground motions is indicated as a sufficient loading level that liquefies part of the column, but not the entire column. Further analysis at a range of applicable void ratios (from dense, medium dense, and loose soil) demonstrate the model's ability to show a differentiation in response as a function of void ratio – including an increase in likelihood of liquefaction when the density of the soil is decreased. These comparisons are shown in Figure 12.

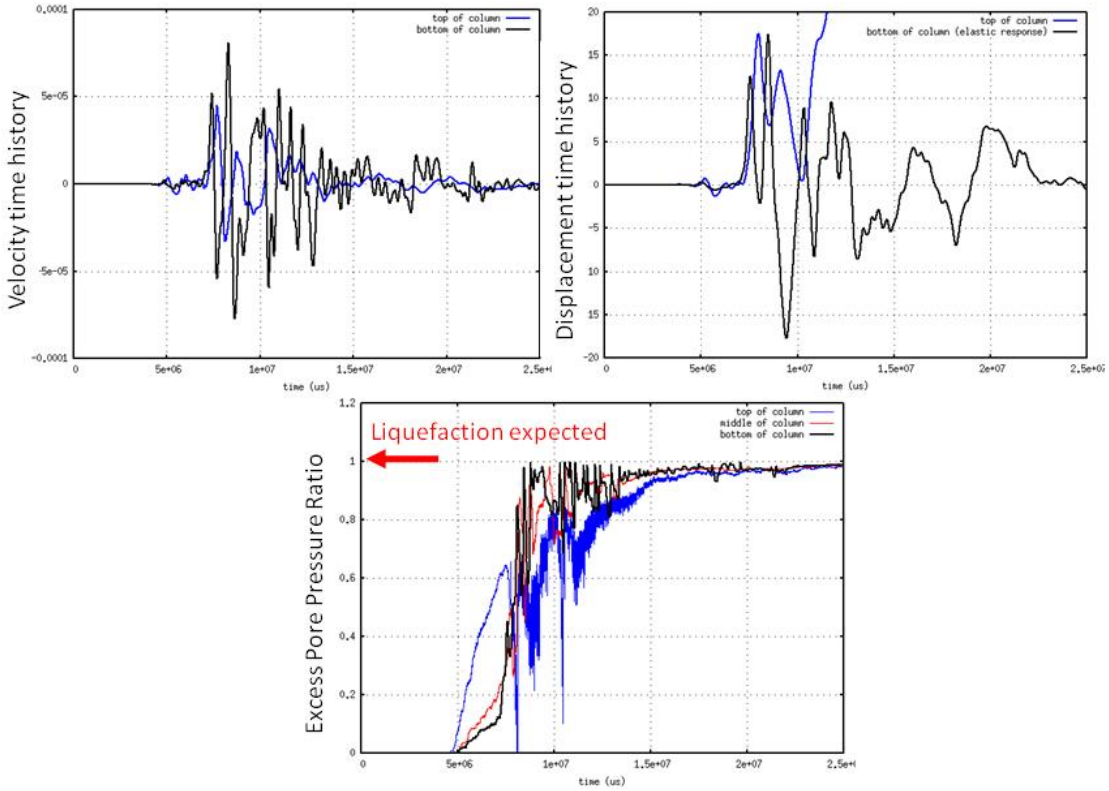

Figure 8: Soil column response to Kobe ground motion for e=0.735.

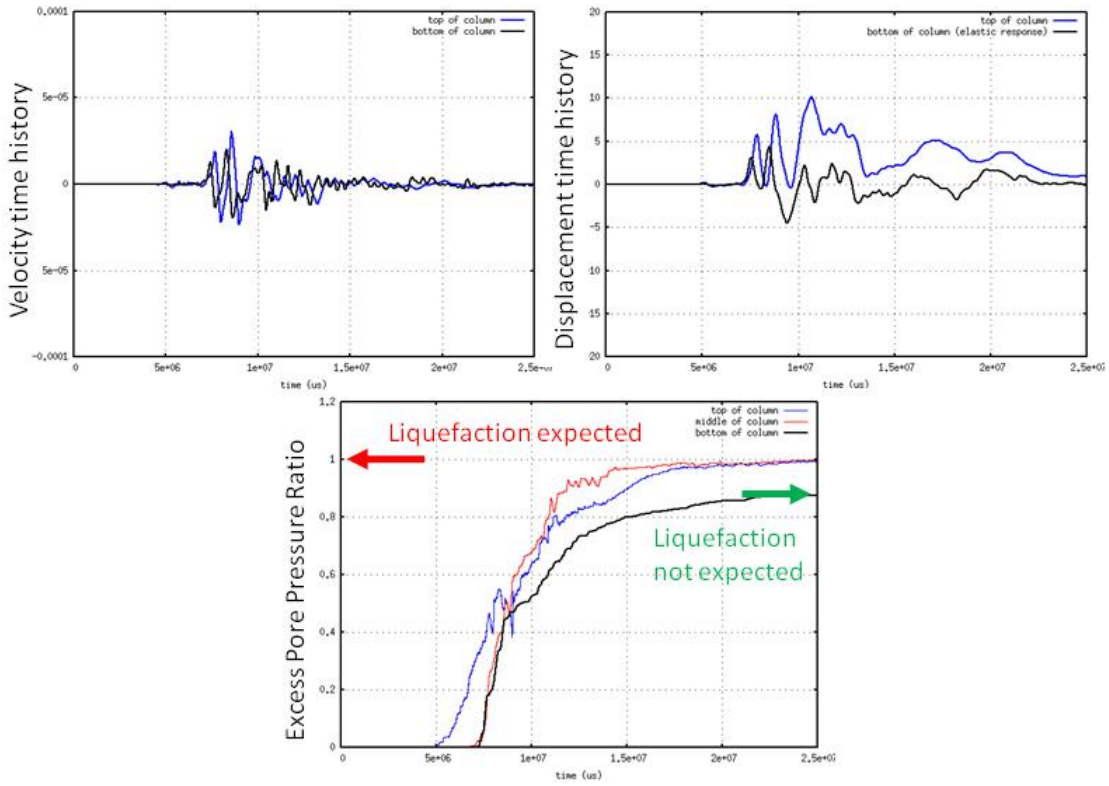

Figure 9: Soil column response to Kobe ground motion, scaled by 0.25, for e=0.735.

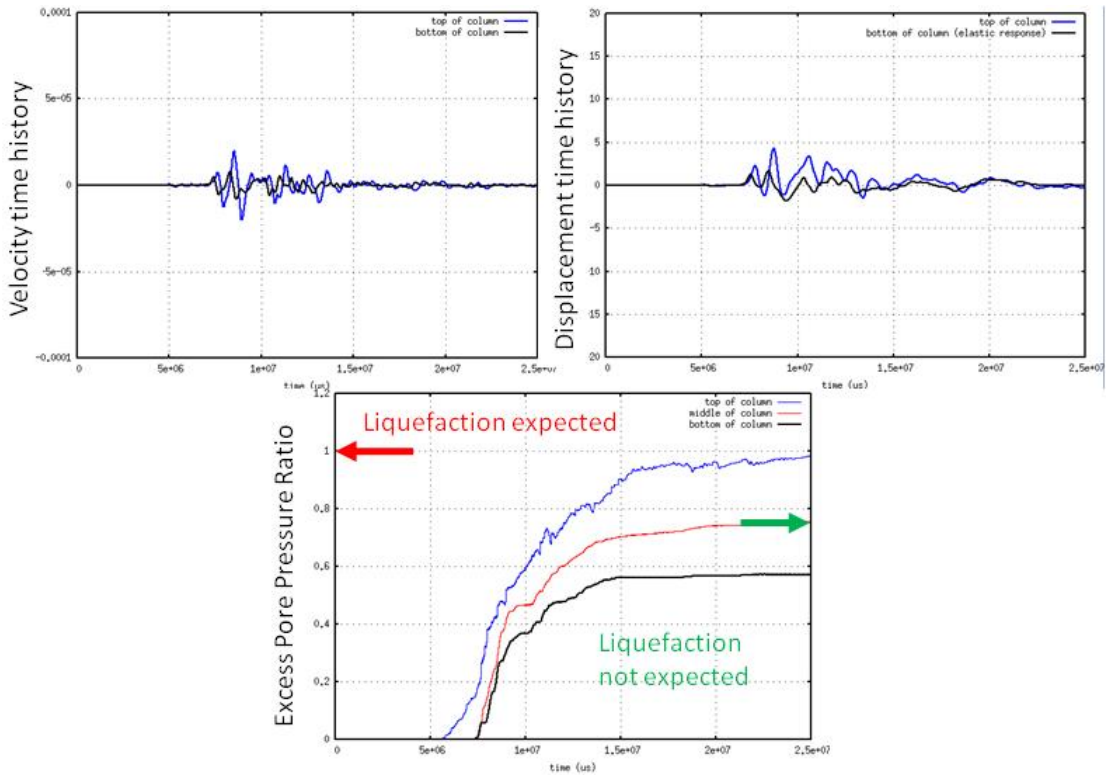

Figure 10: Soil column response to Kobe ground motion scaled by 0.1 for e=0.735

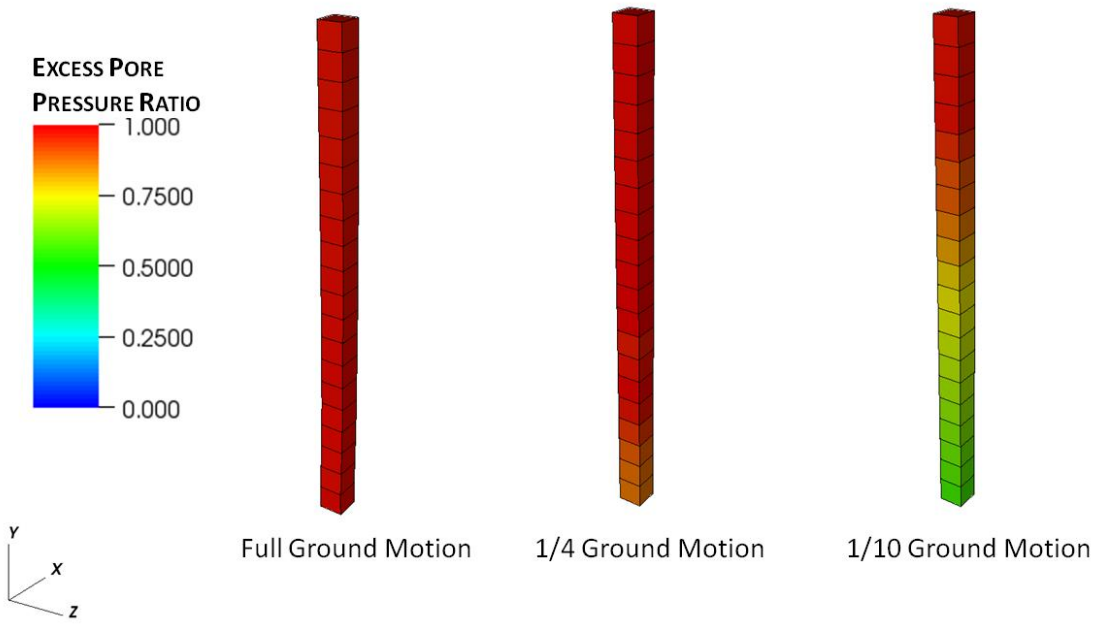

Figure 11: Soil column model comparison shows various levels of liquefaction when the ground motion is scaled

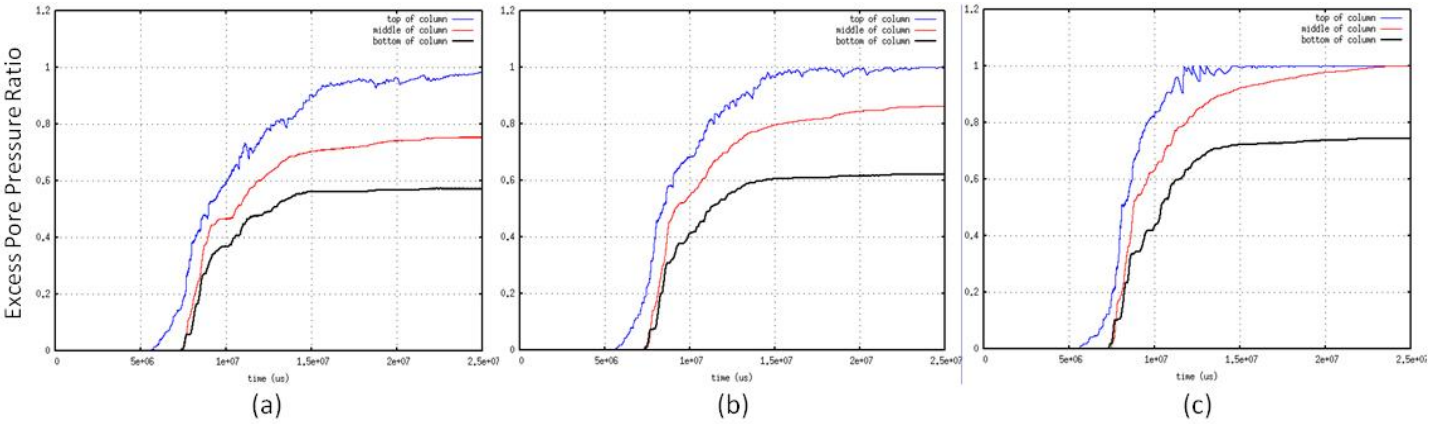

Figure 12: Time histories of Excess Pore Pressure Ratio for a range of void ratio, e, demonstrate that the likelihood of liquefaction increases when the void ratio increases and the soil is less dense. In the following figures, (a) has a void ratio, e=0.735, and a density, ρ=1.95 g/cm^3; (b) e=0.833, ρ=1.9 g/cm^3; and (c) e=0.907, ρ=1.87 g/cm^3.

Boundary Condition Uncertainty and Seismic Loading

Previous studies using LLNL's finite element structural analysis code, DYNA3D, included a comprehensive analysis of the range of loading and boundary condition uncertainty [6]. Throughout this dissertation, a range of problem geometries, mesh refinements, and boundary conditions was investigated. This research gives specific recommendations for the most robust way to set up and run a finite element analysis problem of a seismic event. This includes using a force boundary condition on the nodes of a soil island (which have been computed from the seismic acceleration time history), and boundary conditions that are non-reflecting at the base of the soil island and symmetric at the outer edges. The top surface of the soil model is a free surface.

All of the work in this previous study is based on a linear soil model and it was done in a different finite element code. Although we expected to follow the recommendations of the aforementioned work, it was important that we first check to see the same model behavior and understand the implication of applying a plastically dissipating sand model in place of a linear one.

Soil Island Model and Seismic Loading

In order to verify the previous work performed in DYNA3D with the current version of ALE3D, the exact soil island model and loading that was presented in the dissertation [6] was developed into an ALE3D model. Figure 13 shows a schematic of the model which consisted of 29,998 elements and measures 1040 m^2 and 520 m deep. The figure also shows the deconvolved ground motion data that was used in the dissertation.

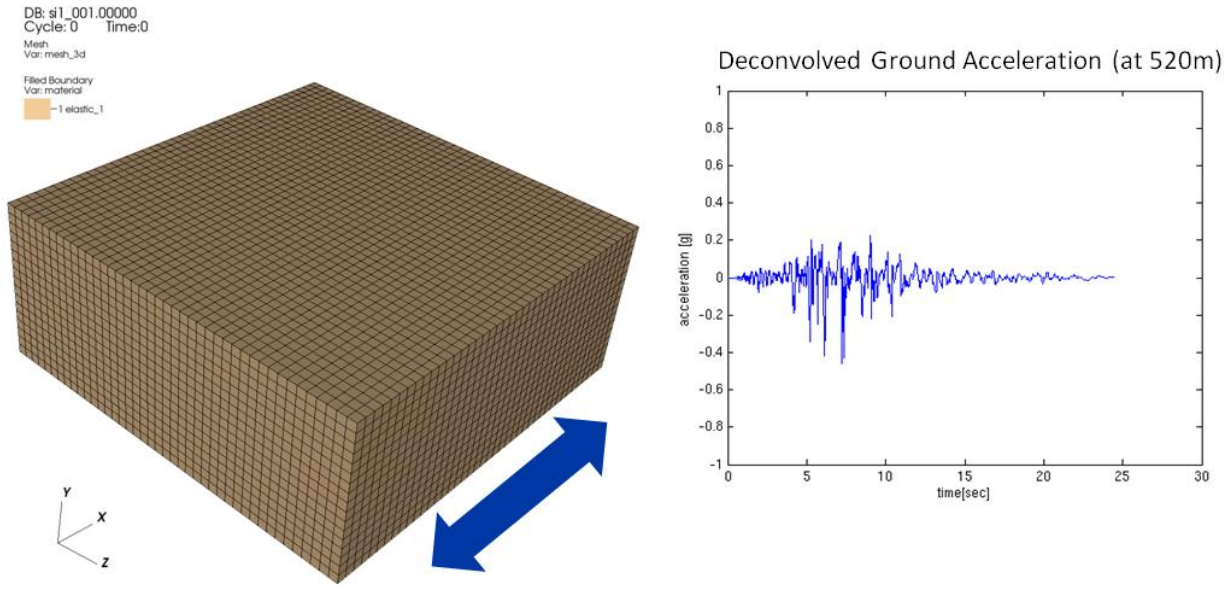

Figure 13: Elastic soil model applied to verify ALE3D response with previous work [6] – ground motions come from the US Bureau of Reclamation.

We followed the methodology of the previous work and derived an equivalent nodal force loading condition. This compensates for the nodal force which is computed and applied by the algorithms of the non-reflecting boundary condition and it is expected to give an equivalent ground acceleration response at the top of the soil island. This loading gives the equivalent response to the velocity loading and it is compatible with the non-reflecting boundary condition at the base of the soil island. The non-reflecting boundary condition is found to be significant in the previous work because the elastic soil propagates (and reflects) seismic shear waves and the load doesn't have a mechanism to leave the problem domain without the non-reflecting boundary. Just as in the previous work, we discovered that the loading from the two time histories are compatible, and that they diverge at ~750,000 us (0.75 s) – the time it takes for the acoustic wave to reflect off the bottom surface and come back to the free surface of the soil island.

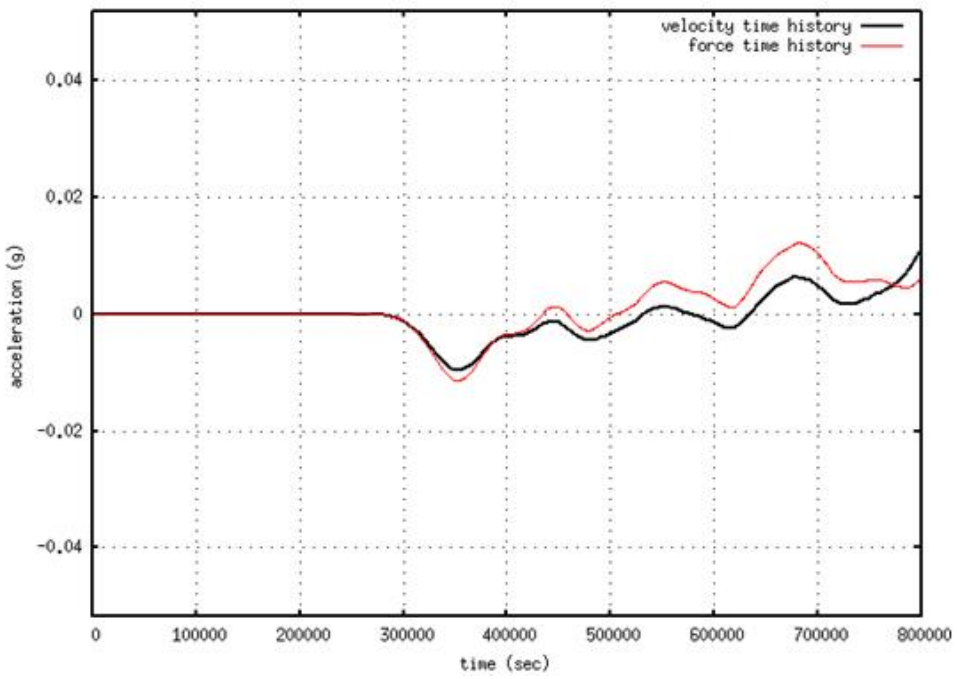

Figure 14: Acceleration time history at the top of a soil island when the loading comes from the measured velocity compared with the force that has been derived from the acceleration time histories.

However, this model differs from the previous work because we are using ALE3D. In DYNA3D, the non-reflecting boundary condition accounts for both pressure and shear waves, thus the compensation routine for seismic velocity shear loading with a force works by adding back the nodal force that would otherwise be removed by the non-reflecting boundary. On the other hand, ALE3D, given its typical application in the hydrodynamic regime, only accounts for pressure or compression wave reflection. Equations 2 and 3 show the forces developed by the non-reflecting boundary conditions of the two codes DYNA3D and ALE3D respectively, side by side. It is clear from these equations that the implementation of non-reflecting boundary conditions is not equivalent between the two codes.

$$F_z = \dot{z}_{gc}(t) A_i \rho \sqrt{\frac{K + \frac{4}{3}G}{\rho}}$$

$$F_x = \dot{x}_{gc}(t) A_i \rho \sqrt{\frac{G}{\rho}} \qquad \{2\}$$

$$F_z = \dot{z}_{gc}(t) A_i \rho \sqrt{\frac{G}{\rho}}$$

$$F_y = -mc \frac{\partial yd}{\partial n} n_y$$

$$F_x = 0 \qquad \{3\}$$

$$F_z = 0$$

Without a mechanism in ALE3D to compensate for the force that is removed by the non-reflecting shear wave (because it is not removed) and therefore no work-around to properly transmit a seismic wave though the loading surface, we were looking at a code development

effort to implement new boundary conditions - unless it is apparent that the boundary condition is not important in the case of this new material implementation.

Throughout our study we had noticed that the new SANISAND non-linear model was extremely dissipative (as is expected with a model that reproduces the behavior of sand), so we did a few scoping studies to see if an acoustic wave in the SANISAND model would even be influenced by a reflection off the boundary. In the study, we applied a large displacement to the bottom of the column and looked at the response of the top. Figure 15 shows the results of a comparison between a linear soil model and the SANISAND model. These results were developed using the model shown in Figure 7. The results show that, indeed, transmitting boundaries are essential for the seismic loading in an elastic material (Figure 15(b)), however the sand model dissipates the energy sufficiently that the effects of boundary reflection appear to be negligible (Figure 15(a)). We also suspect that the lack of a mechanism in ALE3D to reflect shear waves is a likely contributor to this effect. With the results of this study in hand, it was concluded that a code development task to modify the behavior of ALE3D's non-reflecting boundary condition to include shear waves was not required for this capability development project.

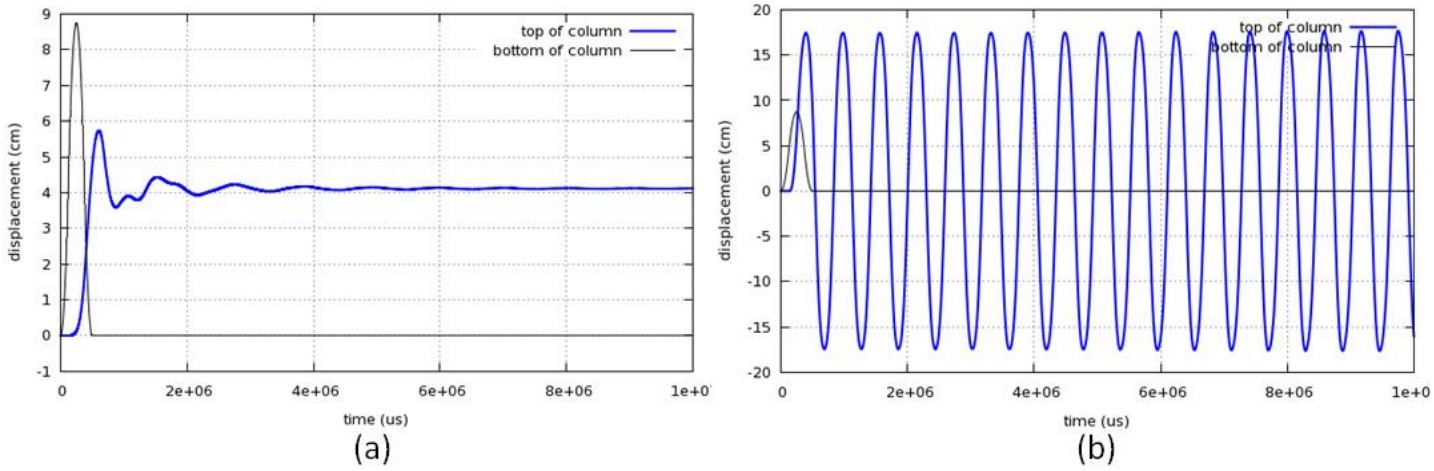

Figure 15: Comparison of displacement time histories at the top of a soil island when (a) SANISAND and (b) linear material models are loaded with a sharp velocity pulse at the base.

Soil Island Model and Boundary Condition Uncertainty

The soil island model with an elastic material representation (presented in the previous section) has been applied on a range of studies to help us understand the influence of boundary conditions on the seismic propagation of a soil island. This model was supplemented by inserting a massive structure at the free surface. Our primary focus was to quantify the effects of using a symmetry, nodal constraint (fixity), or periodic (also by nodal constraint) boundary condition at the edges of the problem, and also the effect of fixed constraint in the gravity loading direction. As with all other studies, the seismic load comes from scaling the 1995 Kobe ground motions.

Our results show that both the ground displacements at the surface of a soil model and the extent of liquefaction do not seem sensitive the boundary conditions that were considered. Figure 16 shows these results for the case when symmetry is compared with nodal constraint in the direction perpendicular to the surface. The almost exact correspondence that results is expected. Figure 17 shows a comparison between the derived Excess Pore Pressure Ratio (EPPR) that is realized for a case with a symmetry boundary condition and a periodic boundary condition which constrains the X-direction nodes to move together. Again, any differences in the results are undetectable in a global fringe plot.

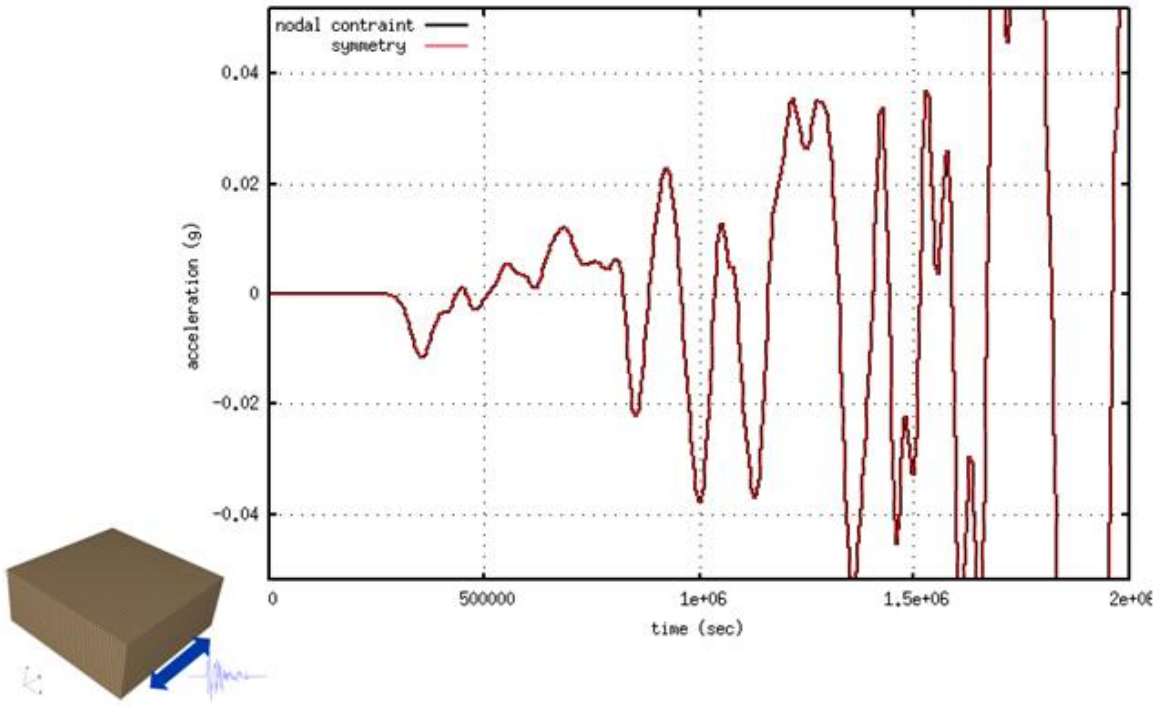

Figure 16: Comparison of acceleration time histories at the free surface for a case with nodal constraint (black line) and symmetry (red line) boundary conditions. Differences between the histories are indistinguishable.

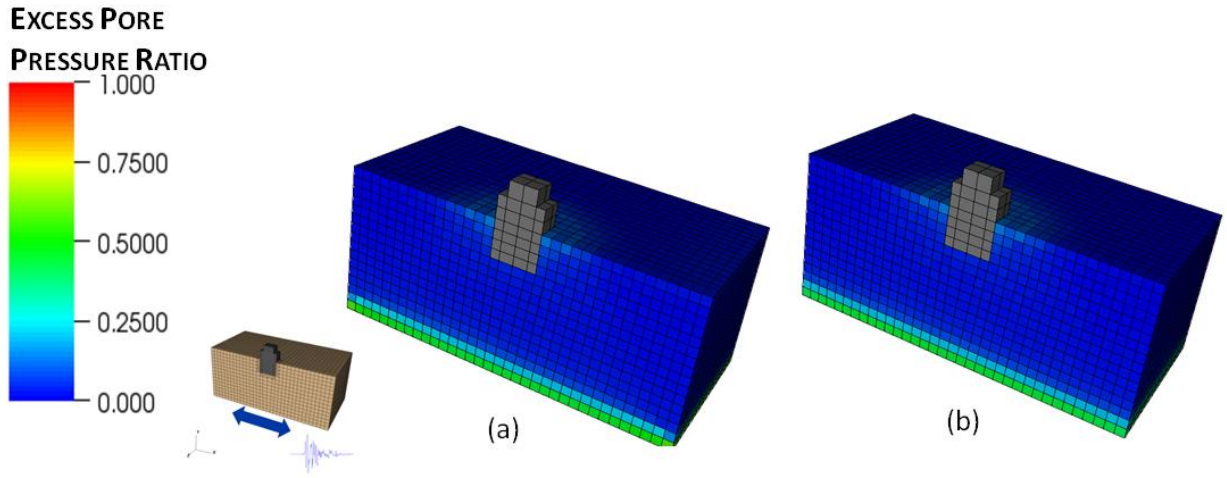

Figure 17: Comparison of Excess Pore Pressure Ratio in the soil island when (a) symmetry and (b) periodic boundary conditions are applied. Differences between the cases are indistinguishable.

We further investigated boundary conditions by comparing the differences in surface acceleration when the Y-direction (gravity direction) nodes are fixed. Naturally, fixity is required for the duration of the problem to ensure that the gravity body force develops compression and hydrostatic pressure, not rigid-body displacement. Figure 18 shows the comparison of constraining all gravity-direction nodes with only those on the bottom surface, as calculated by the elastic soil island without a structure. There is a small amount of long-time drift when all nodes are constrained; however the behaviors both closely match the unconstrained condition. Moving forward, the constraints shall be on the bottom surface only, so that shear dilation (which is included in the SANISAND model) is not inhibited.

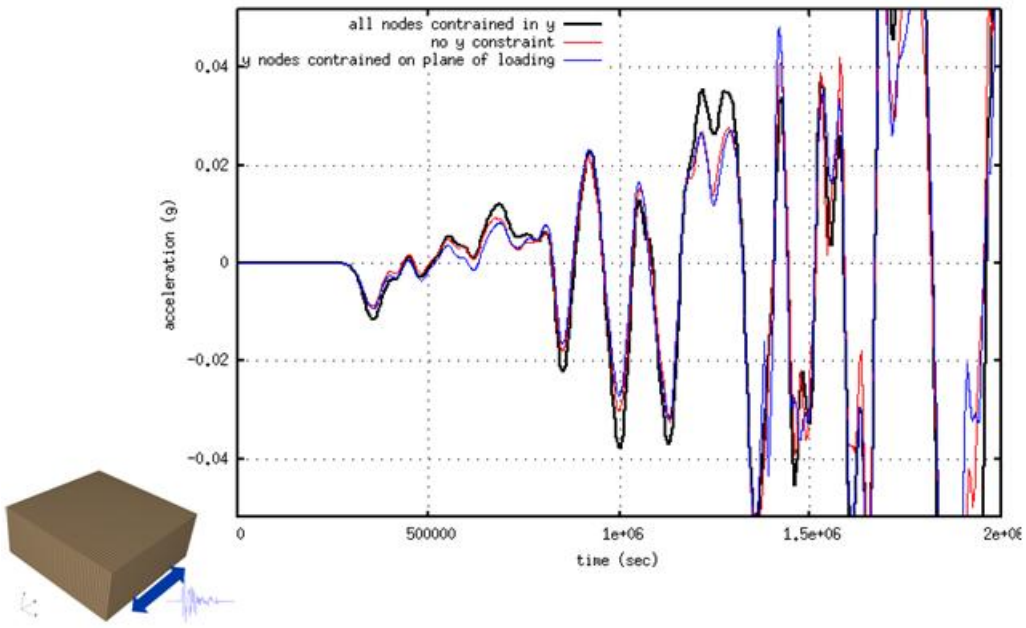

Figure 18: Comparison of Y (gravity) direction fixity shows slight differences between the choices of boundary conditions.

3-dimentional "Generic Reactor" Model

Previous sections described our understanding of the SANISAND model implementation and the boundary and load condition uncertainties. The final test for the integrated capability is the implementation of more representative reactor geometry. Figure 19 shows the latest model which incorporates the approximate moment resisting components of the concrete shear wall structure and includes the additional mass from a 1 in thick steel containment vessel. The model includes 10 m resolution to accommodate frequencies between 2 and 10 Hz. There are 6200 elements total and it takes approximately 8 hours on 32 processors to run 10 sec. of static initialization and 30 sec. of seismic loading. An alternative model was also developed which divides up the soil layer into 10 layers so that the void ratio of the soil could be varied to account for the more dense soil deeper in the island – this model has the same number of elements and takes over 10 hours for a 10 sec. static initialization and 30 sec. of seismic loading. An extra case was run with model to look at a 20 sec. static initialization.

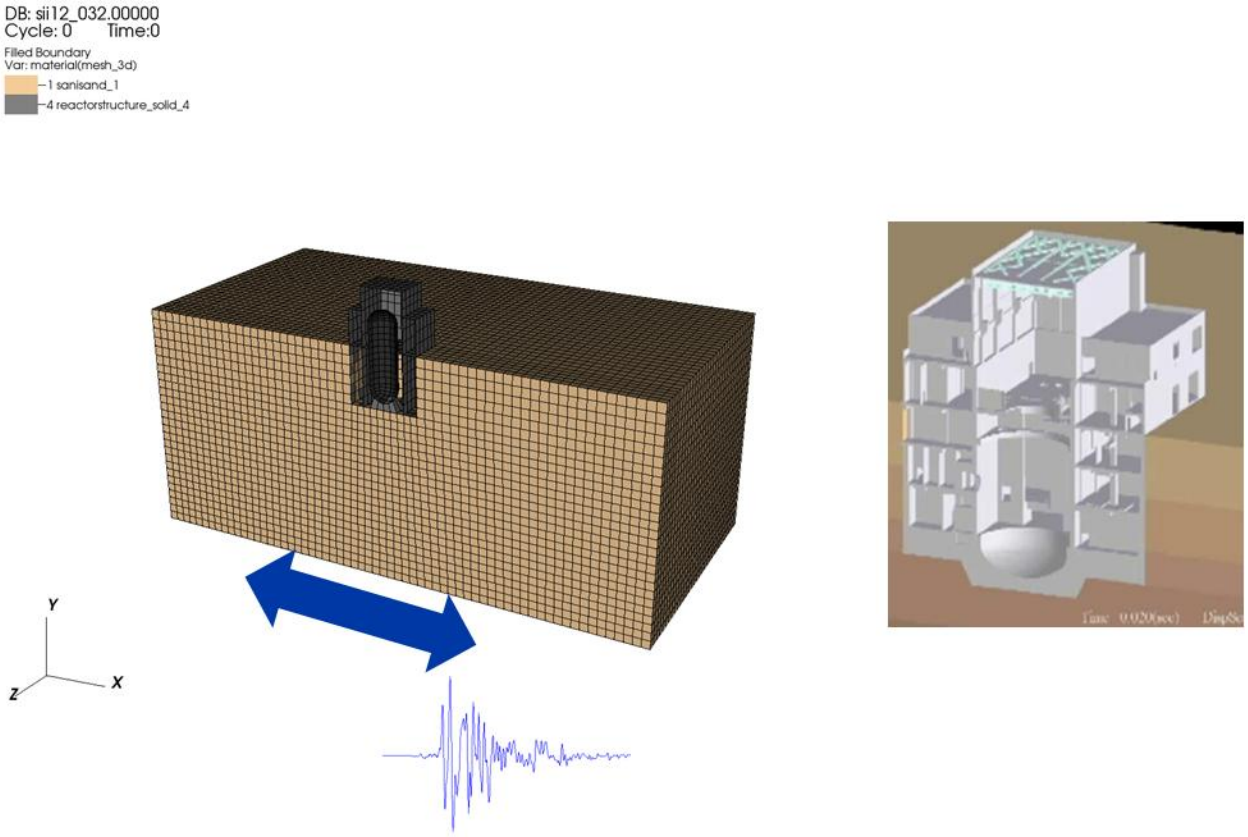

Figure 19: 3-dimensional representation of generic nuclear reactor and soil island used to test the SANISAND model.

Figure 20 shows a comparison of the hydrostatic pressure of the three models at the end of the static initialization. This comparison shows that there are only small differences between the models. Increasing the density with depth by varying the void ratio through layers of soil only accounted for an increase in pressure of 7% at depth. Adding 10 seconds to the static initialization only increased the pressure at depth by 2% and it increased the run time by almost 4 hours on 16 processors.

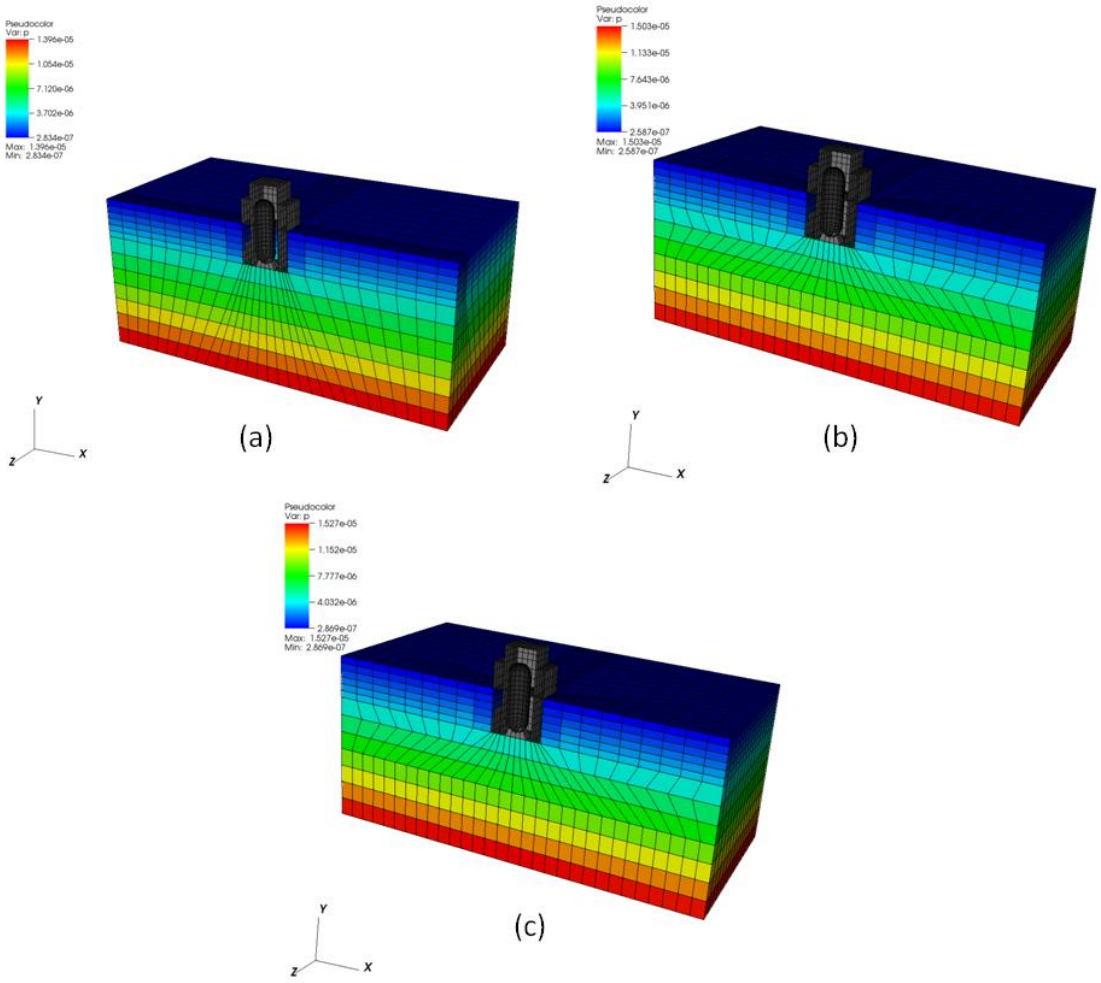

Figure 20: Comparison of pressures after static initialization for three cases: (a) uniform void ratio soil, (b) variable (decreasing) void ratio with depth, and (c) case (b) with twice the duration of static initialization. Note: the legends are slightly different, but all within 7% (peak pressure is 1.396e-5, 1.503e-5, and 1.527e-5 Mbar for a, b, and c respectively).

Comparisons of Excess Pore Pressure Ratio also show that there is little difference in the likelihood of liquefaction in the cases run (which look at void ratio/in situ density and static initialization influences). In fact, the non-linear model seems to dissipate much of the damage in the layer of soil which is being loaded – even when liquefaction doesn't occur. In the first two cases of Figure 21 there is little difference in the regions of the soil island which are expected to experience liquefaction – regardless of the increase in density at depth and increased pressure.

The last calculation shows a case where no liquefaction is expected anywhere in the soil island. It is noted from this result that the soil island methodology of loading with a deconvolved ground motion is likely flawed because the SANISAND model is almost always non-linear and it will tend to dissipate much of the soil damage in the layer which is loaded – regardless of whether the layer liquefies.

We can conclude from this that seismic ground motions for the model must be propagated from a known source or measurement, and not deconvolved from an epicenter measurement. This can only be achieved by increasing the extent of the soil island and/or coupling to a seismic wave propagation code (e.g. WPP [1])

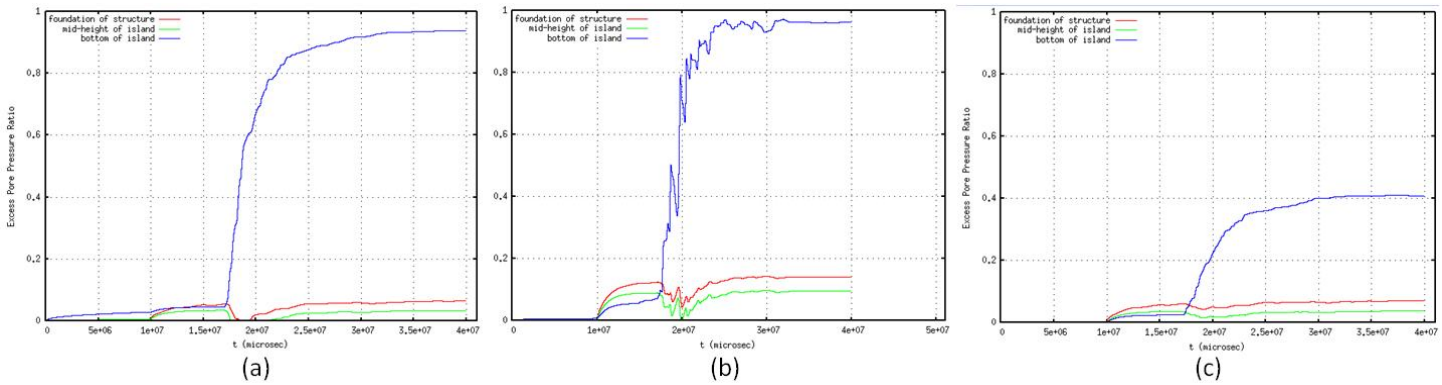

Figure 21: Comparison of Excess Pore Pressure Ratio (likelihood of liquefaction) for the case when: (a) there is uniform void ratio, (b) decreasing void ratio with depth, and (c) 80% reduction in the seismic loading. Note: oscillations in (b) as opposed to the smooth curves in (a) and (c) are likely from discrepancies in the way the tracers were set up in ALE3D.

CONCLUSIONS AND PATH FORWARD

As part of the capability development discussed here, the project team implemented a novel non-linear soil model, SANISAND, which has been developed for cyclic (seismic) loading and parameterized for relevant in-situ sand. Through a series of complex evolution equations and material parameters, this model enabled the team to have the capability to predict the onset of liquefaction for a range of test cases. This model shows great promise in moving the project forward to develop high-fidelity predictive models for Performance-Based Design (PBD).

In this study and throughout this report, numerous computational geometries have been discussed which test certain physical aspects of the seismic response model. These models show that there is a robust capability that should be validated and could be applied to problems of interest (e.g. Tokyo Electric Power Company's Kashiwazaki-Kariwa Nuclear Reactor Facility during the 2007 M6.6 Niigata-ken Chuetsu Offshore Earthquake event as well as future events).

The next phases of this work will focus on improving the computational accuracy and efficiency of the seismic modeling capability by coupling water flow equations (Darcy's Law) to account for pore pressure dissipation post-event, validating the model with experimental centrifuge data on sand from colleagues at UC Davis, applying implicit solution techniques, and collaborating our work and experience with the International Atomic Energy Agency (IAEA) and the Japanese Atomic Energy Agency (JAEA) as part of a growing international collaboration.

The long-term project goals are to develop a modeling framework that demonstrates a fully-coupled, high-fidelity, and robust capability to model seismic events and structural response within LLNL's finite element codes. This capability can be applied to evaluate existing designs, as well as optimize new and novel design strategies that increase the seismic safety of reactors and reduce the risk of accidents following a seismic event. This will also position LLNL to remain the leader in Performance-Based Design of nuclear reactor facilities as permitted by the International Building Code.

REFERENCES

1. Appelo, D., K. McCandless, S. Nilsson, A. Petersson, B. Sjogreen. *User's Guide to the Wave Propagation Program (WPP)*. LLNL technical report: UCRL-SM-230257 (2007).
2. ASCE/SEI 7-05, *Minimum Design Loads for Buildings and Other Structures*, American Society of Civil Engineers (2005).
3. ASCE/SEI 43-05, *Seismic Design Criteria for Structures, Systems, and Components in Nuclear Reactor Facilities*, American Society of Civil Engineers (2005).
4. *International Building Code (IBC)*, International Code Council, Inc. (2006).
5. Nichols, A. *Users manual for ALE3D: An arbitrary Lagrange/Eulerian 3D code system*. LLNL technical report: UCRL-MA-152204 Rev 6 (2007).
6. Noble, C. *Finite Element Techniques for Realistically Simulating the Seismic Response of Concrete Dams*, Submitted in partial satisfaction of the requirements for the degree of Doctor of Philosophy, 2007.
7. Parsons, I., J. M. Solberg, R. M. Ferencz, M. A.Havstad, N. E. Hodge, A. P. Wemhoff. *Diablo Users Manual*. LLNL technical report: UCRL-SM-234927 (2007).
8. Taiebat, M. and Y. Dafalias, *SANISAND: Simple anisotropic sand plasticity model*, Int. J. Numer. Anal. Meth. Geomech. 2008; 32:915-948.
9. USGS website. www.usgs.gov
10. U.S. Nuclear Regulatory Commission, *A Performance-Based Approach to Define the Site-Specific Earthquake Ground Motion*. Regulatory Guide 1.208. March 2007.